frontiers | Frontiers in Materials

TYPE Original Research
PUBLISHED 20 April 2023
DOI 10.3389/fmats.2023.1163919

OPEN ACCESS

EDITED BY
Domenico De Tommasi,
Politecnico di Bari, Italy

REVIEWED BY
Raffaella Rizzoni,
University of Ferrara, Italy
Enrico Masoero,
Cardiff University, United Kingdom

*CORRESPONDENCE
Zenghui Zhao,
skd992945@sdust.edu.cn

RECEIVED 14 February 2023
ACCEPTED 03 April 2023
PUBLISHED 20 April 2023

CITATION
Zhao Z, Dong Z, Gao X and Liu H (2023), Splitting failure and deformation evolution of the red argillaceous siltstone disc in the high humidity environment. *Front. Mater.* 10:1163919. doi: 10.3389/fmats.2023.1163919

Splitting failure and deformation evolution of the red argillaceous siltstone disc in the high humidity environment

Zenghui Zhao[1,2]*, Zhongtai Dong[1], Xiaojie Gao[1] and Hao Liu[1]

[1]College of Energy and Mining Engineering, Shandong University of Science and Technology, Qingdao, China, [2]State Key Laboratory of Mining Disaster Prevention and Control Co-founded by Shandong Province and the Ministry of Science and Technology, Qingdao, China

The failure mechanism of weakly cemented soft rock under water-rock coupling effect is extremely complex. To reveal the tensile failure of red argillaceous siltstone in high humidity environment, five kinds of disc samples with different water contents were obtained through maintenance in constant temperature and humidity oven. The Brazilian test was carried out to reveal the variation characteristics of splitting behavior of rock samples in high humidity environment. Detailed analysis was conducted on the evolution law of stress-strain relationship and mechanical parameters under five different water contents. Combined with the DIC (Digital Image Correlation) investigation, the displacement evolution patterns of samples with different water content and loading stages were analyzed. Results show that he macroscopic mechanical parameters such as tensile strength and elastic modulus of weakly cemented red sandstone samples under water environment are negatively parabolic correlated with the increase of water content. The moisture content has an important influence on the disc splitting failure mode, forming the main fracture along the radial direction of loading, and showing a local crushing area in the loading area, and the crushing area increases with the increase of water content. Microstructural variation of red sandstone under a high humidity environment is the main reason for its deterioration of macroscopic mechanical properties.

KEYWORDS

high humidity environment, weakly cemented red sandstone, disc splitting, mechanical behavior variation, meso–macro-degradation

1 Introduction

Jurassic and Cretaceous weakly cemented soft rocks are widely present in coal mining projects in western China. Their typical characteristics are low strength, poor cementation, easy to mud, and collapse upon contact with water, resulting in extremely unstable mechanical properties. (Zhao et al., 2020a; Zhao et al., 2020b). In mine roadway engineering, additional deformation and stress field disturbance of local surrounding rocks will be caused directly or indirectly in the excavation space due to factors such as construction water and groundwater storage, which will cause long-term stability and safety issues (Bibhash et al., 2020; He, 2014; Yang et al., 2017). Therefore, disclosing the mechanical variation characteristics caused by water in weakly cemented soft rock has become a key and difficult topic in the study of the water–rock interaction, and it is also a crucial problem to be urgently solved in various engineering applications.

The water environment has a significant effect on the physical, chemical, and mechanical properties of rocks, which has attracted the attention of researchers (Hu et al., 2020; Yan et al., 1991; Zhao et al., 2023). The tensile strength of rocks is an important parameter to evaluate the stability of surrounding rocks (Isrm, 1978; Satoch, 1987; Guo et al., 1993; Yu et al., 2002; Markides et al., 2012), and a large amount of achievements have been made in the study of the tensile strength of rocks under the water–rock effect. The researchers found that the water environment has a significant weakening effect on the tensile strength of rocks and a significant influence on the deformation by disc splitting experiments under different water contents or saturated states (Huang et al., 2015; Hawkin et al., 1992; Vasarhelyi et al., 2003; You et al., 2011). Erguler et al. (2009) obtained the attenuation degree of rock strength and elastic modulus under saturated conditions by uniaxial compression and tensile tests on different types of clay mineral rock samples and devised an empirical model to evaluate the hydrophilicity of rocks based on the test results. Xiong et al. (2011) found that saturated water decreased the cohesion of different rock samples to varying degrees, but the friction factor remained identical, indicating that cohesion was a structural parameter and the friction factor was a material parameter. You et al. (2011) found that the effect of the saturated state on tensile strength of rocks is mainly manifested in the weakening of cohesive force, while the effect on compressive strength is also affected by the internal friction coefficient and pore pressure, and further analyzed the influence of water on tensile strength of sandstone. The effect of water on tensile strength of rocks involves a process from microscopic structure variation to macroscopic mechanical property degradation (Chen et al., 2010; Deng et al., 2017). Combined with AE (acoustic emission) monitoring and SEM investigation, many scholars have obtained the microstructural evolution and fracture energy evolution process of different saturated states under the splitting state (Jiang et al., 2013; Huang et al., 2015).

Domestic and overseas scholars have carried out systematic research on water softening and micro-structural variation of rocks, but most of them focus on different moisture contents or saturation states. Few studies have been carried out on the mechanical behavior of weakly cemented soft rock disc splitting caused by water diffusion in a high humidity environment, as well as the microscopic damage degradation, mineral composition, and water absorption softening of soft rock. Therefore, in this study, the Brazilian splitting test is carried out for samples cured in the high humidity environment. Combining digital image processing technology with SEM, this study reveals the mechanical behavior of disc splitting damage in weakly cemented soft rocks in the high humidity environment, as well as the degradation mechanism and variation law at the micro- and macro-levels.

2 Sample preparation and experimental methods

2.1 Sample preparation

The splitting samples were taken from the red argillaceous siltstone thin layer in the Gansu mine. The processing of the rock sample strictly implements "standard for rock test methods" suggested by the International Society for Rock Mechanics (ISRM, 1978), and the rock sample is processed into a disc with a diameter of 50 mm and a thickness of 25 mm. In the thickness direction, the diameter and parallelism errors of the end face of the rock sample are less than 0.1 mm, and the deviation between the end face and the axis of the rock sample is less than 0.25°.

In order to analyze the influence of the high humidity environment on the splitting failure characteristics, it is necessary to prepare a variety of rock samples with different moisture contents, and the specific steps are as follows: 1) the rock samples with large density differences are eliminated by the acoustic test; 2) the rock sample is dried for 24 h to constant weight, cooled in the dryer to room temperature, and then weighed; 3) the rock specimens are then placed in a constant temperature and humidity oven for curing, with a humidity of 100% and a temperature of 20°C. The curing times are set to 2, 6, 10, and 15 days, respectively; 4) the rock samples are taken out at the end of maintenance, and the moisture content (the ratio between the mass of evaporable water and the dry sample mass) is then calculated. Brazilian splitting rock samples with different moisture contents are shown in Figure 1.

Five kinds of water content rock samples were selected for experimental analysis. The rock sample number and corresponding water content are shown in Table 1.

FIGURE 1
Brazilian disc samples.

TABLE 1 Number of split rock samples and moisture content.

Number	ω/%	Curing time/d
PW1	0	0
PW2	2.9	2
PW3	5.6	6
PW4	7.8	10
PW5	8.6	15

2.2 Experimental method

The Brazilian splitting test was carried out on the AG-X250 experimental system. The surface deformation field of rock samples with different moisture contents was analyzed by digital speckle and digital image processing technology. The test equipment and test method are shown in Figure 2.

The specific experimental steps are as follows: 1) measuring points are sprayed on the surface of the prepared specimens and installed on the digital speckle monitoring system, 2) the prepared specimens are placed in the arc-shaped fixture, and the pressure plate of the testing machine was adjusted to ensure that the specimen is uniformly loaded and the rock sample is in the center of the Shimadzu testing machine's pressure head, and 3) the displacement loading method is adopted, and the loading rate is set at 0.005 mm/s for the experiment. The specimen is loaded until it is broken, and the experimental data and the failure phenomena of the rock are recorded.

3 Results and discussion

3.1 Variation of mechanical behavior in the high humidity environment

Repeated experiments were carried out in this test, and three rock samples for each water content were tested. Figure 3A shows the stress–strain curves of the samples under five moisture contents, each containing three sets of test data. In addition, error bars for tensile strength and elastic modulus are plotted in Figure 3B. Due to the drying treatment of dry rock samples, the peak strength has a relatively large dispersion. The greater the water content of the sample, the more obvious the variability of the stress–strain curve, such as the *PW*5 group. The deformation of samples experienced four stages: the compaction stage, linear elastic stage, yield plastic stage, and post-peak drop stage. With the increase in the moisture content, the tensile strength of the sample gradually decreases, and the elastic modulus and peak strain also exhibit a decreasing trend. This is due to the increase in water content caused by water absorption in a high humidity environment and the expansion of mineral components after water absorption, which destroys the internal microstructure and reduces the mechanical properties of the sample during the fracturing process. The detailed mechanical parameters of the Brazilian splitting test for red sandstone with different water contents are shown in Table 2.

Figure 4 shows the variation of tensile strength with water content. The tensile strength of red sandstone decreases roughly in a parabolic manner with an increase in the water content. The relationship between the tensile strength σ_t (MPa) and water content ω (%) of red sandstone with varying water contents can be fitted as follows:

$$\sigma_t = 1.2186 - 15.26\omega + 78\omega^2 \quad (1)$$

Rabat et al. (2020) carried out the splitting strength test of calcarenite building stones with different water contents and proposed a negative three-parameter exponential function between tensile strength and w, which is similar to the result shown in Eq. 1.

3.2 Effect of moisture content on the splitting deformation field

At present, most Brazilian splitting tests are carried out under the single condition of mechanical loading, and there are few reports on the study of the splitting failure characteristics and surface deformation fields of soft rocks under high humidity. The following analysis of the surface deformation fields of red

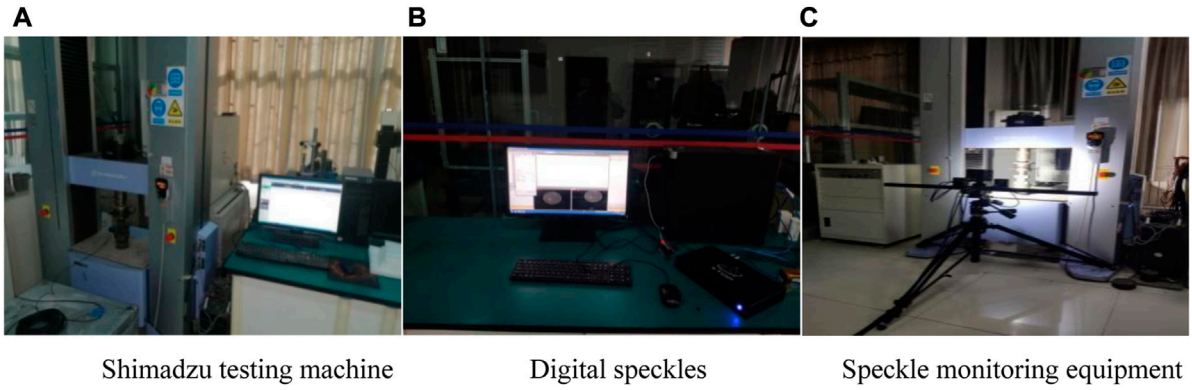

FIGURE 2
Test equipment and monitoring method. **(A)** Shimadzu testing machine, **(B)** digital speckles, and **(C)** speckle monitoring equipment.

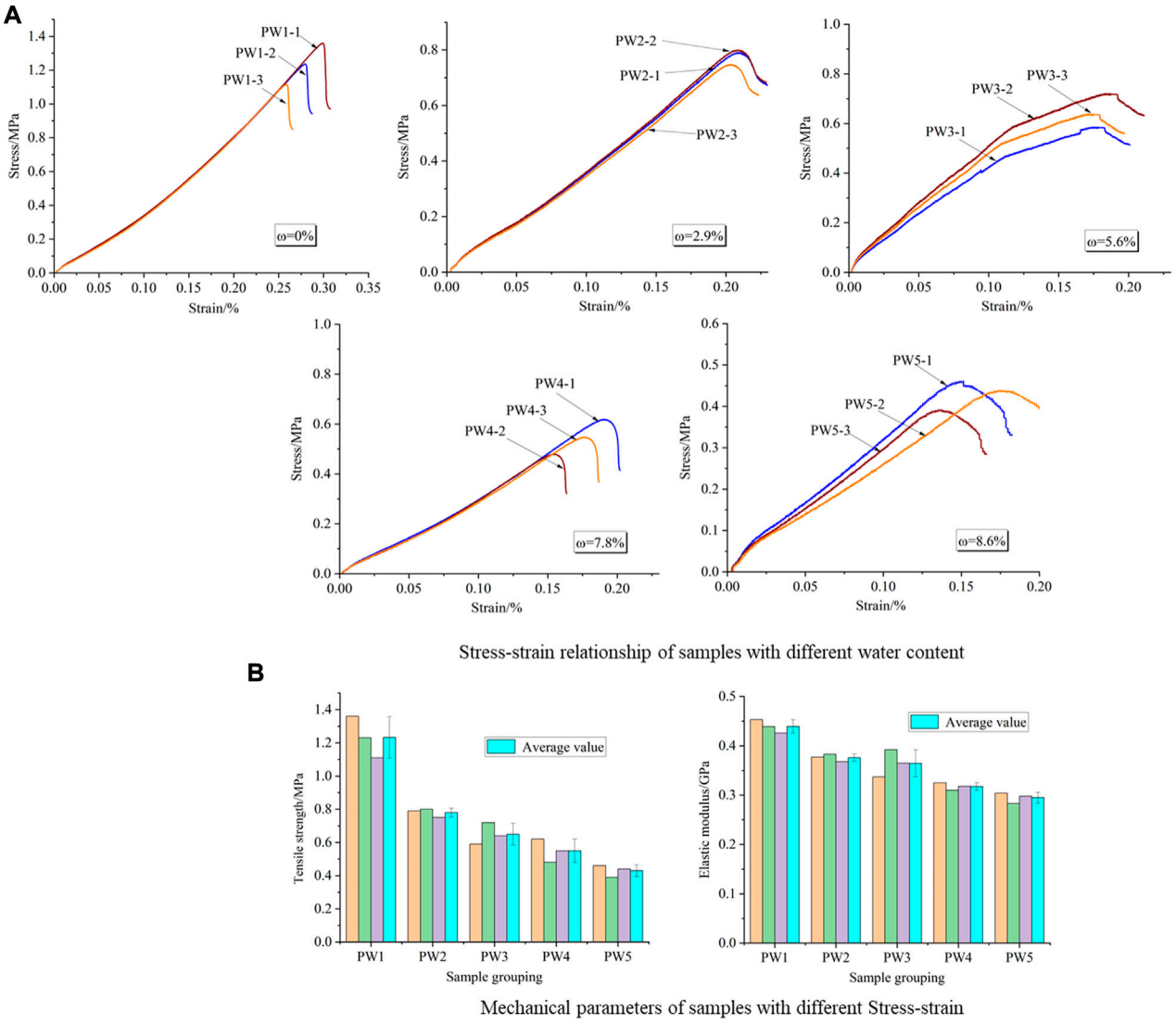

FIGURE 3
Stress–strain and mechanical parameter analyses of samples with different water contents. **(A)** Stress–strain relationship of samples with different water contents. **(B)** Mechanical parameters of samples under different water contents.

sandstone with different water contents using a digital speckle system aims to reveal the effect of water content on the deformation characteristics of splitting.

The digital speckle measurement system is shown in Figure 5, which is mainly composed of a camera, light source, and computer. Before the beginning of the test, the rock sample surface was sprayed with speckle measuring points, and then the processed rock sample was placed under the pressure head of the Shimadzu testing machine. In order to make the obtained image have a stable gray value, it is necessary to ensure that the optical spindle of the camera is perpendicular to the surface of the rock sample and provides a stable light source. After the experiment started, the digital speckle monitoring system transmitted and stored the acquired digital image in the computer. When the speckle images were processed, the load and time information of the deformed image were obtained by loading the data in the control testing machine.

The strain evolution during loading is extremely complex, in which the strain in the *x*-direction is closely related to the splitting failure. In order to reveal the strain evolution rules in the *x*-direction at different loading stages under the same water content and to compare the strain distribution characteristics at the same loading characteristic points under different water contents, Figure 6 marks five strain monitoring points on the stress–strain curves with different water contents, which correspond to the compaction stage, the elastic stage, the elastoplastic demarcation point, the plastic stage, and the peak point.

Figure 7A shows the evolution process of the horizontal stress at the center point and the *x*-direction strain field in the whole splitting process of dry rock samples. When the rock sample is in the compaction stage, the evolution of the strain field on the disc surface is disordered due to the closure of the internal microstructure. When the rock specimen enters the elastic stage

TABLE 2 Mechanical parameters of samples with different water contents.

Group	ω/%	Failure load/kN			Tensile strength/MPa			Elastic modulus/GPa		
		Value	Average	Deviation/%	Value	Average	Deviation/%	Value	Average	Deviation/%
*PW*1-1	0	2.67	2.42	10.3	1.36	1.24	9.68	0.453	0.439	3.19
*PW*1-2		2.41		−0.41	1.23		−0.81	0.439		0
*PW*1-3		2.18		−9.91	1.11		−10.48	0.426		−3.19
*PW*2-1	2.9	1.39	1.53	−9.15	0.79	0.78	1.28	0.377	0.376	0.27
*PW*2-2		1.73		13.1	0.80		2.56	0.383		1.86
*PW*2-3		1.47		−3.92	0.75		−3.84	0.368		−2.13
*PW*3-1	5.6	1.16	1.28	−9.37	0.59	0.65	−9.23	0.337	0.365	−7.67
*PW*3-2		1.41		10.2	0.72		10.77	0.392		7.39
*PW*3-3		1.26		−1.56	0.64		−1.54	0.367		0.54
*PW*4-1	7.8	1.22	1.08	12.9	0.62	0.55	12.73	0.325	0.318	2.20
*PW*4-2		0.94		−12.9	0.48		−12.73	0.310		−2.52
*PW*4-3		1.08		0	0.55		0	0.320		0.63
*PW*5-1	8.6	0.90	0.84	7.14	0.46	0.43	6.98	0.304	0.295	3.05
*PW*5-2		0.80		−4.76	0.39		−9.30	0.283		−4.07
*PW*5-3		0.82		−2.38	0.44		2.32	0.298		1.02

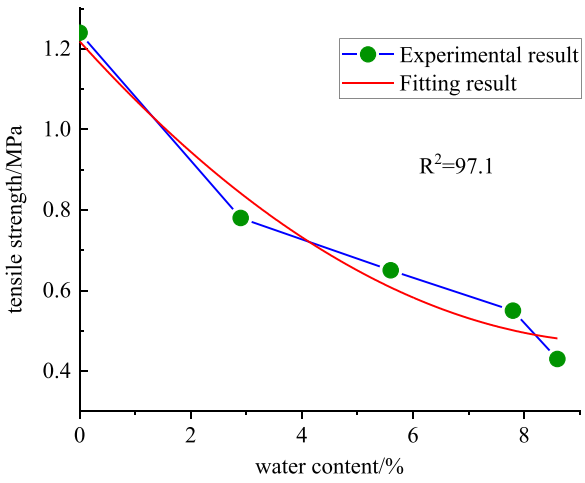

FIGURE 4
Influence of water content on tensile strength of red sandstone in the Brazilian splitting test.

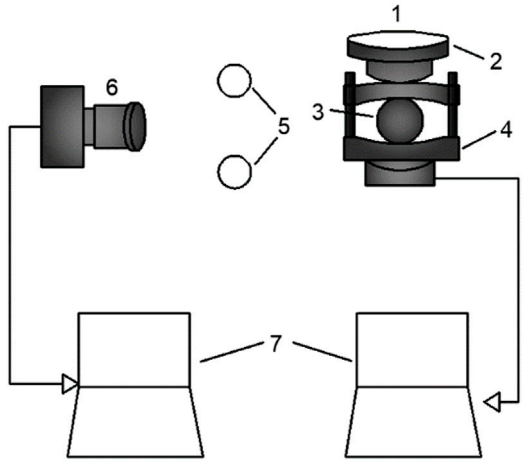

FIGURE 5
Brazilian disc deformation field test system. 1—pressure equipment; 2—pressure sensor; 3—red sandstone disc; 4—arc fixture; 5—light source; 6—camera; 7—computer.

after the compaction stage, displacement concentration areas is found at the critical points of the two stages, appearing in the upper left and lower right positions of the disc, as shown in disc a and disc b; then, with the progress of the elastic stage, the strain changes in the upper left and lower right of the disc are more intense, and the strain field of the disc at the junction of the elastic and plastic stages shows a relatively obvious left–right boundary, as shown in disc c; with the progress in the plastic yield stage, the concentrated position of the strain field gradually shifts to the left and right ends of the disc, and the concentration degree is more intense. A strain band that approximately coincides with the stress loading direction gradually appears in the axial position of the disc, and the crack begins to develop at this time, as shown in disc d; with further loading, the specimen enters the post-peak failure stage. At the peak point, large deformation of the left and right regions of the disc leads to the continuous expansion of the crack, and the central axis position of disc e gradually appears as blank points. This is

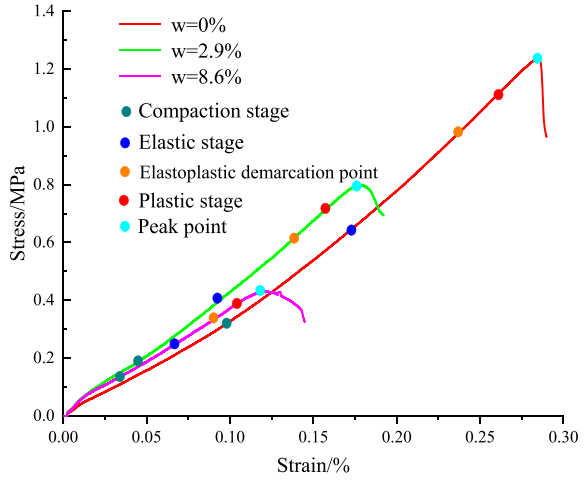

FIGURE 6
Strain watching points under different water contents.

because the excessive development of cracks leads to the lack of monitoring points for digital speckles.

Figure 7B compares the evolution of the *x*-direction strain field during the loading process of the disc with different water contents. The five graphs show the strain distribution nephogram of the same deformation stage under different water contents, which correspond to the compaction stage, the elastic stage, the elastoplastic demarcation point, the plastic stage, and the peak point. In the process of loading, due to the influence of end face stress concentration, the strain at the upper and lower ends accumulates and develops first. With further loading, the strain accumulation area and value on the disc gradually increase and gradually develop near the loading line of the disc, which roughly coincides with the loading direction, and then the strain near the loading line of the disc increases rapidly. Finally, the strain concentration area on the disc forms an extreme strain band near the loading line, which runs through the upper and lower ends of the disc and divides the disc into two parts with roughly equal areas.

Combined with Figure 8, it can be observed that although the failure modes of circular specimens with different water contents are roughly in line with the direction of stress loading, the distribution of the strain concentration areas is not the same during their strain evolution processes. Figure 7A shows that in the initial stage of loading, the strain concentration area of the specimen under dry conditions is roughly distributed in the center and loading end of the disc. According to the analytical solution of the stress field of the disc (Zhao et al., 2020b), the compressive stress at the loading end of the disc is much greater than the tensile stress produced by the rock Poisson effect, and the ratio of compressive and tensile stresses reaches its minimum in the center of the disc. The specimen initially fails in tension in the center of the disc, and the crack gradually develops and expands toward the loading end, gradually developing and penetrating into the strain concentration zone in the disc strain field and ultimately forming an extreme strain band. Later, with the increase in the water content, the location of strain concentration on the disc varies, and it shows roughly that with the increase in the water content, the concentration area shifts from the center of the disc to both ends. The reason for this is that the diffusion range of moisture in the specimen differs with varying water contents, and the dry–wet interface generated by the diffusion of moisture causes stress concentration during the loading process, resulting in the formation of strain concentration zones, which affects the initial failure position.

4 Failure characteristics of the splitting disc with different moisture contents

4.1 Macroscopic failure mode

According to the Griffith failure criterion, the Brazilian splitting test is considered effective only when the fracture gradually extends from the center of the disc specimen to the loading end. However, during the experiment, the disc is placed between the upper and lower indenters of the testing machine and directly loaded radially, leading to local stress concentration near the loading end and preferential shear failure at the end. Due to different diffusion depths of the humidity field under different water contents, the splitting failure of the samples exhibits different characteristics.

Figure 8 shows the failure patterns of red sandstone under different water contents. The stress field of specimens cured in a high humidity environment changes due to humidity diffusion and expansion deformation, and the higher the moisture content, the greater the range of humidity impact will be. Unlike dry specimens, the horizontal tensile stress and compressive stress of the disc increase with the increase in external humidity in the range of the humidity influence zone, which has been theoretically analyzed in the previous studies (Zhao et al., 2020b), as shown in Figure 9. The content of clay minerals in red sandstone is relatively high. Due to the diffusion of humidity, the internal structure of the sample becomes weak to absorb water, the internal cemented minerals expand and dissolve, the structure between mineral particles is destroyed, and the mechanical properties of the rock sample are reduced.

4.2 Discussion on the micromechanism of the moisture absorption effect

Red argillaceous siltstone is characterized by weak cementation, which is rich in clay minerals and calcareous cement. In the natural dry state, the microstructure is dense, with fewer internal pores and cracks and good integrity. However, in a high humidity environment, as the sample absorbs water, the mineral particles are eroded and dissolved by the cement, weakening the bonding force between the particles. The weakening of the cementation structure directly leads to an increase in the porosity and a decrease in the density of the sample. The lubrication of pore water also reduces the cementation strength to a certain extent. After the weak cementation structure is eroded by water, the surface water film becomes thicker and easily forms a water wedge together with pore water (Zhang et al., 2020). Under the action of the water wedge and capillary pressure, the original weak cementation structure is prone to tensile deformation, as shown in Figure 10,

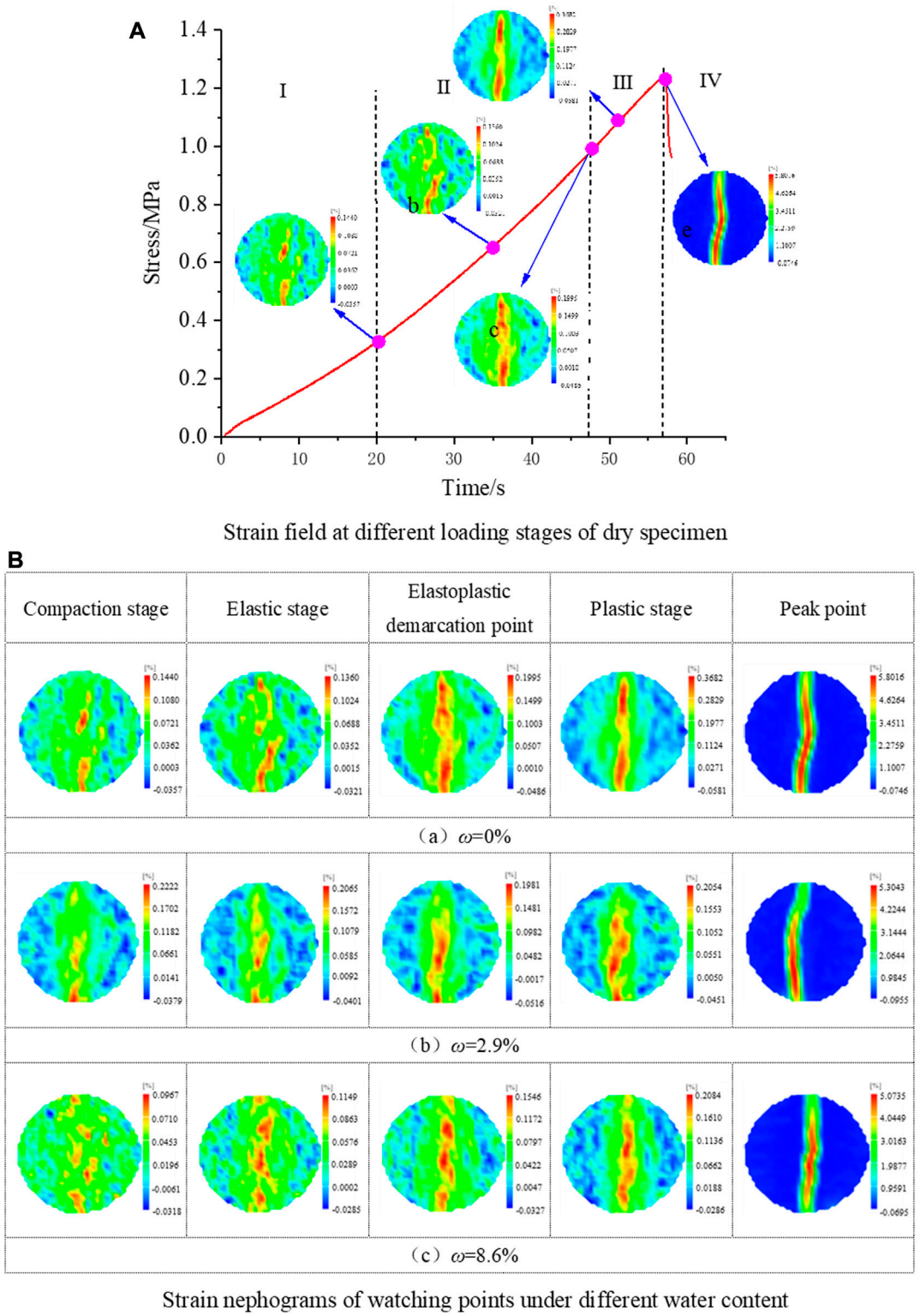

FIGURE 7
Evolution of the horizontal strain in the splitting disc with different water contents. **(A)** Strain field at different loading stages of dry specimen. **(B)** Strain nephograms of watching points under different water contents.

leading to an increase in the distance between cemented particles and a decrease in cementation strength. When there is a combined action of load and water, the presence of pore water pressure increases the lateral stress level, strengthens the Poisson effect, and accelerates the damage to the cementation structure. The weak cementation structure of red argillaceous siltstone is the

10.3389/fmats.2023.1163919

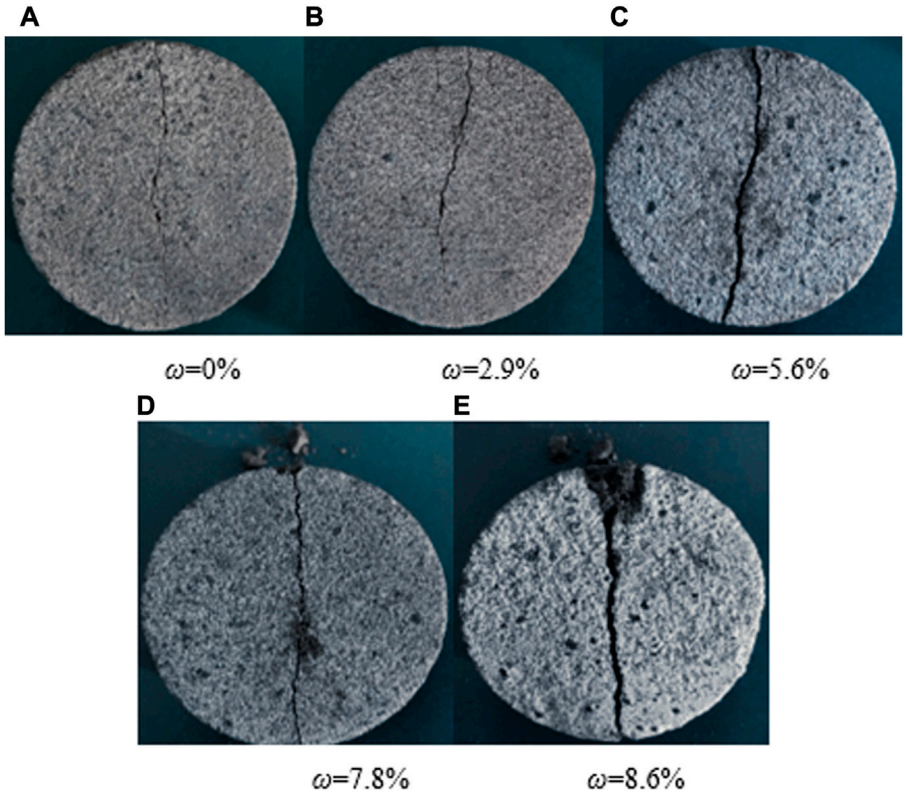

FIGURE 8
Brazilian splitting failure modes of red sandstone with different water contents. **(A)** ω = 0%, **(B)** ω = 2.9%, **(C)** ω = 5.6%, **(D)** ω = 7.8%, and **(E)** ω = 8.6%

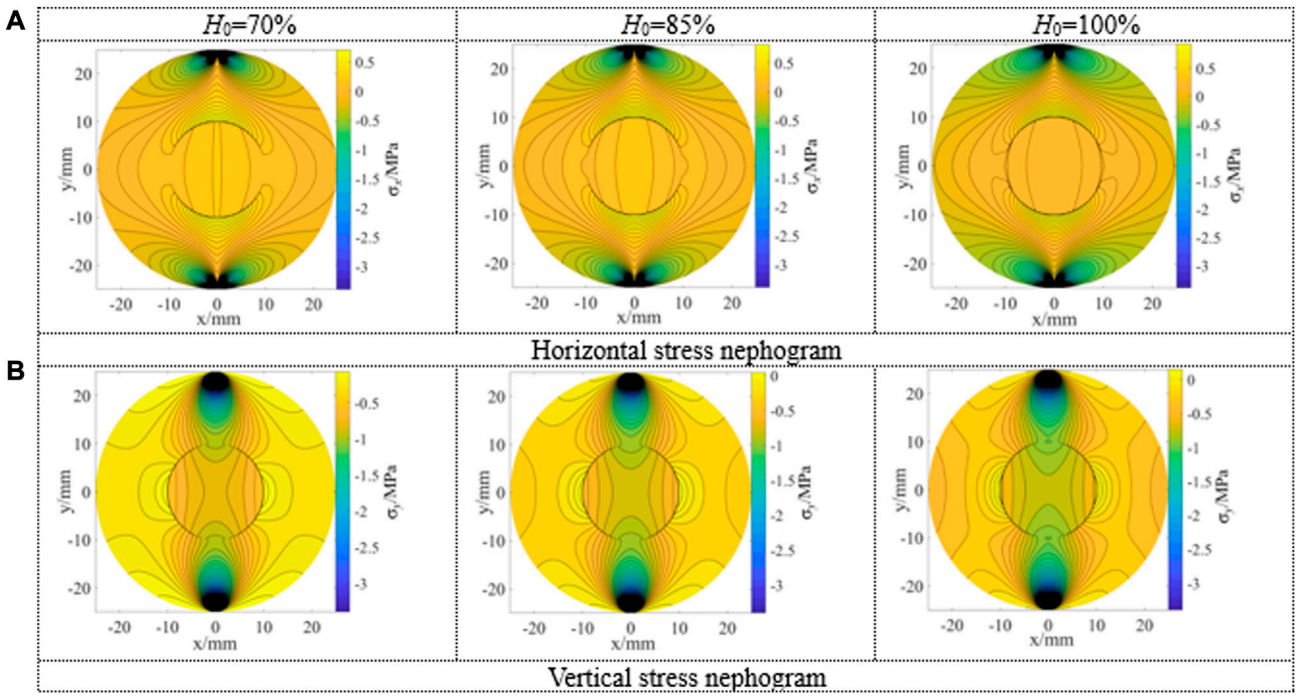

FIGURE 9
Stress nephogram of the disc under the influence of the humidity field (Zhao et al., 2020b). **(A)** Horizontal stress nephogram. **(B)** Vertical stress nephogram.

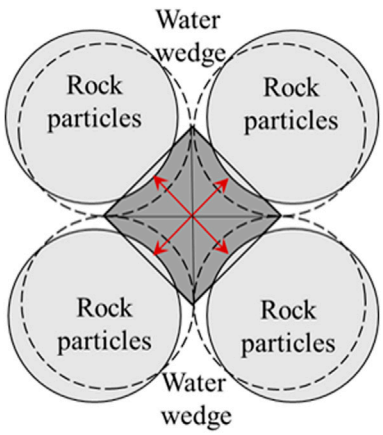

FIGURE 10
Tensile failure of weakly cemented structures after water absorption.

main reason for its decreased ability to resist deformation and load after water absorption.

5 Conclusion

The Brazilian splitting test was carried out on weakly cemented red argillaceous siltstone taken from the Gansu coal mine. Combined with the microscopic structure observation, the effect of water content on macroscopic mechanical characteristics and microscopic damage of disc specimens was revealed. The main conclusions are drawn as follows:

(1) During the Brazilian splitting test, the mechanical parameters such as tensile strength and elastic modulus of the sample decrease as the water content increases. Although the cracks in the disc specimens split roughly and coincide with the direction of the loading line, the diffusion range in specimens with different water contents is different. The dry–wet interface caused by the diffusion of the water content causes stress concentration during the loading process, resulting in strain concentration areas, which will affect the initial failure position.
(2) Brazilian splitting failure modes of red sandstone vary with the water content. During the splitting process, the disc forms a main crack that runs through the upper and lower ends of the disc and approximately coincides with the loading direction, and a local crushing area appears at the loading place of the disc specimen. The size of the crushing zone increases with the increasing water content.
(3) The tensile failure of micro-weak cementation structures is the main reasons for the deterioration of the macroscopic mechanical properties of the samples. With the increase in water content, the dissolution of cementitious materials and the formation of etching pores will significantly weaken the connection between particles, and the disordered arrangement tends to become loose. Under the combined action of mechanical loading and water, the initiation and propagation of microcracks are promoted. As microscopic defects expand and connect, significant changes in the macroscopic structure morphology occur. In the follow-up study, the SEM test will be conducted to deeply reveal the microstructural changes and mechanical mechanisms of water absorption degradation of weakly cemented soft rocks in high humidity environments.

Data availability statement

The original contributions presented in the study are included in the article further inquiries can be directed to the corresponding author.

Author contributions

ZZ: methodology, formal analysis, data curation, validation, software, and writing—original draft. ZD: writing and editing and validation. XG: investigation and supervision. HL: resources and software.

Funding

This paper was supported by the National Natural Science Foundation of China (Nos. 51774196) and the National Natural Science Foundation of China and Shandong Province Joint Program (U1806209).

Conflict of interest

The authors declare that the research was conducted in the absence of any commercial or financial relationships that could be construed as a potential conflict of interest.

Publisher's note

References

Chen, Y., Cao, P., Pu, C. Z., Liu, Y. K., and Li, N. (2010). Experimental study of effect of water-rock interaction on micro-topography of rock surface. *Rock Soil Mech.* 31 (11), 3452–3458. doi:10.16285/j.rsm.2010.11.052

Deng, H. F., Zhang, Y. C., Li, J. L., Wang, W., and Zhi, Y. Y. (2017). Effect of moisture content on splitting tensile strength of layered sandstone. *Chin. J. Rock Mech. Eng.* 36 (11), 2778–2787. doi:10.13722/j.cnki.jrme.2017.1175

Erguler, Z. A., and Ulusay, R. (2009). Water-induced variations in mechanical properties of clay-bearing rocks. *Int. J. Rock Mech. Min. Sci.* 46 (2), 355–370. doi:10.1016/j.ijrmms.2008.07.002

Guo, H., Aziz, N. I., and Shmidt, L. C. (1993). Rock fracture toughness determination by the Brazilian test. *Eng. Geol.* 33 (3), 177–188. doi:10.1016/0013-7952(93)90056-i

Hawkin, A. B., and Mcconnell, B. J. (1992). Sensitivity of sandstone strength and deformability to changes in moisture content. *Q. J. Eng. Geol.* 25 (2), 115–130. doi:10.1144/gsl.qjeg.1992.025.02.05

He, M. C. (2014). Progress and challenges of soft rock engineering in depth. *J. China Coal Soc.* 39 (8), 1409–1417. doi:10.13225/j.cnki.jccs.2014.9044

Hu, S. Y., Xiao, C. L., Liang, X. J., Cao, Y. Q., Wang, X. R., and Li, M. Q. (2020). The influence of oil shale *in situ* mining on groundwater environment: A water-rock interaction study. *Chemosphere* 228, 384–389. doi:10.1016/j.chemosphere.2019.04.142

Huang, Y. H., and Yang, S. Q. (2015). Quasi-static loading strain rate effects on saturated limestone based on Brazilian splitting test. *Chin. J. Geotechnical Eng.* 37 (5), 802–811. doi:10.11779/CJGE201505005

ISRM (1978). International society for rock mechanics Suggested methods fordetermining tensile strength of rock materials. *Int. J. Rock Mech. Min. SciGeomechAbstr* 15, 99–103. doi:10.1016/0148-9062(78)90003-7

Jiang, M. J., Chen, H., and Liu, F. (2013). A microscopic bond model for rock and preliminary study of numerical simulation method by distinct element method. *Chin. J. Rock Mech. Eng.* 32 (1), 15–23. doi:10.3969/j.issn.1000-6915.2013.01.005

Kumar, BibhashJagdish Prasad Sahoo (2020). Support pressure for circular tunnels advanced below water bodies. *Tunn. Undergr. Space Technol.* 97, 103214. doi:10.1016/j.tust.2019.103214

Markides, C. F., and Kourkoulis, S. (2012). The stress field in a standardized Brazilian disc: The influence of the loading type acting on the actual contact length. *Rock Mech. Rock Eng.* 45 (2), 145–158. doi:10.1007/s00603-011-0201-2

Rabat, A., Tomás, R., and Cano, M. (2020). Evaluation of mechanical weakening of calcarenite building stones due to environmental relative humidity using the vapour equilibrium technique. *Eng. Geol.* 278 (8), 105849. doi:10.1016/j.enggeo.2020.105849

Satoch, Y. (1987). Position and load of failure in Brazilian test a numerical analysis by Griffith criterion. *J. Soc. Mater. Sci.* 36 (410), 1219–1224. doi:10.2472/jsms.36.1219

Vasarhelyi, B. (2003). Some observations regarding the strength and deformability of sandstones in dry and saturated conditions. *Bull. Eng. Geol. Environ.* 62 (3), 245–249. doi:10.1007/s10064-002-0186-x

Xiong, D. G., Zhao, Z. M., Su, C. D., and Wang, G. Y. (2011). Experimental study of effect of water-saturated state on mechanical properties of rock in coal measure strata. *Chin. J. Rock Mech. Eng.* 30 (5), 998–1006.

Yan, Y. D., Liao, Y. Q., Wu, J. N., and Shi, Y. (1991). Tension resistant strength of rock under confining pressure. *South China J. Seism ology* 11 (2), 1–12. doi:10.13512/j.hndz.1991.02.001

Yang, R. S., Li, Y. L., Guo, D. M., Yao, L., Yang, T. M., and Li, T. T. (2017). Failure mechanism and control technology of water-immersed roadway in high-stress and soft rock in a deep mine. *Int. J. Min. Sci. Technol.* 27 (2), 245–252. doi:10.1016/j.ijmst.2017.01.010

You, M. Q., Chen, X. L., and Su, C. D. (2011). Brazilian splitting strengths of discs and rings of rocks in day and saturated conditions. *Chin. J. Rock Mech. Eng.* 30 (3), 464–472.

Yu, M. H. (2002). Advances in strength theories for materials under complex stress state in the 20th century. *ASME Appl. Mech. Rev.* 55 (3), 169–218. doi:10.1115/1.1472455

Zhang, J. F., Cheng, S. F., Wan, H., Gao, Z., Zhou, F. W., and Zhou, H. W. (2020). Experiment of mesostructure and hydrologic characteristics of weakly cemented soft rocks in western China. *Coal Geol. Explor.* 48 (3), 116–121. doi:10.3969/j.issn.1001-1986.2020.03.017

Zhao, Z. H., Gao, X. J., Chen, S. J., Zhang, M. Z., and Sun, W. (2020b). Coupling model of disk splitting for expansive rock mass in deep storage considering water infiltration. *Energy Sci. Eng.* 8 (9), 3200–3216. doi:10.1002/ese3.729

Zhao, Z. H., Sun, W., Chen, S. J., Feng, Y. H., and Wang, W. M. (2020a). Displacement of surrounding rock in a deep circular hole considering double moduli and strength-stiffness degradation. *Appl. Math. Mech.* 41 (12), 1847–1860. doi:10.1007/s10483-020-2665-9

Zhao, Z. H., Liu, H., Gao, X. J., and Feng, Y. H. (2023). Meso-macro damage deterioration of weakly cemented red sandstone under the coupling effect of high-humidity and uniaxial loading. *Eng. Fail. Anal.* 143, 106911. doi:10.1016/j.engfailanal.2022.106911